ADVANCED MATERIALS
www.advmat.de

Elastomeric Conductive Composites Based on Carbon Nanotube Forests

By *Min Kyoon Shin, Jiyoung Oh, Marcio Lima, Mikhail E. Kozlov,* Seon Jeong Kim,** and *Ray H. Baughman*

Electrically conductive materials capable of substantial elastic stretch and bending are needed for such applications as smart clothing,[1] flexible displays,[2] stretchable circuits,[3] strain gauges,[4] implantable devices,[5] high-stroke microelectromechanical systems,[6] and dielectric elastomer actuators.[7] A variety of approaches involving carbon nanotubes (CNTs) and elastic polymers have been suggested for the fabrication of conductive elastic composites. In particular, diverse active and passive electronic components have been embedded in rubber sheet by several research groups to obtain stretchable electronic devices.[8–10] Sekitani et al. developed rubber-like conductive composites by mixing millimeter-long single-walled carbon nanotubes (SWNTs), an ionic liquid, and a fluorinated copolymer.[11] The stretchability of the resulting composite was enhanced by creating perforated films with a net-shaped structure using a mechanical punching system. Cao et al. fabricated flexible electrodes by incorporating SWNT networks in plastics consisting of polyimide, polyurethane, and polyamic acid films.[12] Although quite successful, these studies indicated that high loading of CNTs (or other conductive additive) was necessary to obtain a highly conducting composite. On the other hand, incorporation of high concentrations of CNTs into an elastic polymer increases the stiffness of the resulting composite and decreases its stretchability.[13] In other words, the significant difference in the Young's modulus of extremely rigid CNTs and the elastic polymer filler makes the creation of a highly stretchable conductive composites a challenging task.

It is known that CNTs can be fabricated into macroscopic assemblies, such as mats (bucky paper), yarns, and fibers that possess useful electrical properties, and that these assemblies can be used for the fabrication of conductive polymer composites. While these assemblies are often more elastic than the individual CNTs, the achievable elastic strain range is still quite limited, normally less than 10%.[14–16] We found that a combination of high stretchability and high electrical conductivity can be obtained for composites prepared from three-dimensional CNT structures, such as CNT forests (vertically aligned arrays of CNTs). Unlike previous methods involving casting CNT/polymer dispersions as a film, our composites were prepared by the direct infiltration of multiwalled carbon nanotube (MWNT) forests with a polyurethane (PU) solution. Using this procedure, we obtained rubber-like forest/PU composites that combined high stretchability with high electrical conductivity. These composites provide highly reversible stress–strain behavior and little degradation of mechanical and electrical properties even when stretched over a wide strain range. The developed preparation procedure appears scalable for material fabrication on an industrial scale, though transition from present batch-based forest growth processes to continuous forest growth processes would be needed for applications that are price sensitive and depend on sheet weight, rather than the area of elastomeric sheet.

The aligned arrays of MWNTs (MWNT forests) used in this study were grown on iron-catalyst-coated silicon wafers using a conventional chemical vapor deposition (CVD) method.[17] Nanotubes in the forests typically had a diameter of about 10 nm; their length could be controlled across a wide range by changing the growth time and other fabrication conditions. The forest-covered area on the substrate used for the preparation of the composites typically had dimensions of about $50 \times 100\ mm^2$; the height of nanotubes in the forest was about 50 μm as determined by the conventional optical microscopy. Since the nanotubes in the forests formed a three-dimensionally interconnected network, the forests were electrically conductive in all directions.

The MWNT forests were infiltrated with a PU solution in *N,N*-dimethylformamide (DMF) using a simple drop-casting procedure, as shown in Figure 1a. The PU used was poly[4,4′-methylene-bis(phenyl isocyanate)-alt-1,4-butanediol/poly(butylene adipate)]. After evaporation of the solvent, we obtained about 250 μm thick forest/PU composite sheets that could be peeled off the underlying Si wafer. Figure 1b shows a photograph of the MWNT/PU composite sheet taken at low magnification. One side of the prepared film facing the substrate (forest side) was black and conductive, and the other side (PU side) was white and insulating. The material was soft, flexible, and highly stretchable in the sheet plane.

Figure 1c shows a SEM image of a cross-section of the composite sheet with the top (~50 μm in thickness) being the forest side and the bottom (~200 μm in thickness) being the PU side. A high magnification image of the forest side is shown in the

[*] Dr. M. E. Kozlov, Dr. J. Oh, Dr. M. Lima, Prof. R. H. Baughman
Alan G. MacDiarmid NanoTech Institute
University of Texas at Dallas
Richardson, TX 75083 (USA)
E-mail: Mikhail.Kozlov@utdallas.edu
Prof. S. J. Kim, M. K. Shin
Center for Bio-Artificial Muscle and Department of Biomedical Engineering
Hanyang University
Seoul 133-791 (Republic of Korea)
E-mail: sjk@hanyang.ac.kr

DOI: 10.1002/adma.200904270

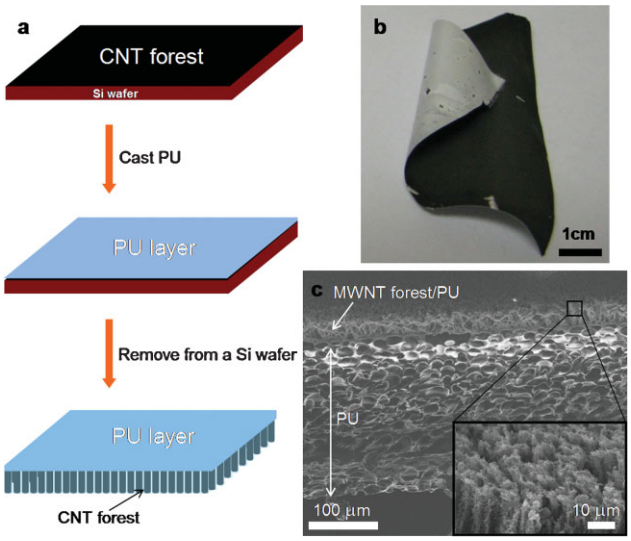

Figure 1. a) Schematic diagram of the preparation method for the forest/PU composite sheet. b) Optical photograph showing opposite sides of the composite sheet. c) SEM image of the sheet cross section. A high-magnification SEM image of the black forest side is shown in the inset.

inset. From Figure 1c and the inset of Figure 1c, we confirmed that the PU polymer completely penetrates into the forest side, and found that the PU layer interconnected with the forest forms a highly porous foam. The overall density of the prepared forest/PU composite was quite low, about 0.43 g cm^{-3}, that can be related to its porous structure (Fig. 1c) created by the evaporation of the solvent upon sample drying. According to our estimate, the MWNT loading in the forest side of the composite shown in Figure 1b was about 5.4% and the overall loading in the layered composite was about 0.1%. Note also that the thickness of the PU layer could be controlled in a quite broad range by variation of infiltration conditions.

This preparation procedure can be easily extended for the fabrication of multi-layer samples by applying another PU or forest layer to the surface of the composite sheet. As a result, sandwich structures of the type forest-PU-forest (conductive on both sides) or PU-forest-PU (conductive layer embedded into insulating PU) can be obtained. The structures retain outstanding elastic properties and high in-plane electrical conductivity. The sandwich structures produced by this method may have applications in highly stretchable electrodes and smart clothing that require either both conducting or insulating sides. Pristine PU sheets were prepared as a reference using the same fabrication conditions as for the forest/PU composite.

For electrical measurements, prepared sheets were cut into about 20 × 3 × 0.25 mm^3 strips. The overall electrical conductivity of the strips was 10–20 S m^{-1} with the conductivity of the forest/PU layer being about 50-100 S/m. The latter is close to the value expected if the pristine MWNT forests grown on Si wafers retained their electrical conductivity upon infiltration. This conductivity is 1–2 orders of magnitude higher than the reported conductivity of composites prepared by loading PU with 5 wt% of MWNT powder (0.052 S m^{-1}[18] and 0.1 S m^{-1}[19]) or 20 wt% of carbon black powder (0.049 S m^{-1}).[20] Note also that the maximum achievable strain at break for the MWNT/PU composite with 5 wt% MWNT loading was only 25%.[18] The commercially available carbon-filled rubbers (Stockwell Elastomerics, Inc., Philadelphia, USA) typically have the conductivity 2–20 S m^{-1}, tensile strength 2–6 MPa, and strain at break 100%–275%. These values are markedly lower than the corresponding values for the prepared forest/PU composites.

The elasticity of the prepared forest/PU composite was evaluated using tensile stress vs. strain measurements (Fig. 2a). The initial Young's modulus and final mechanical strength of this composite calculated from engineering stress–strain curves were about 19.4 MPa and 10.1 MPa, respectively. These values of Young's modulus and strength were 148% and 38% higher, respectively, than for the reference pristine PU sheet (Fig. 2a). This enhancement in modulus and strength indicates substantial penetration of the PU into the nanotube forest, since

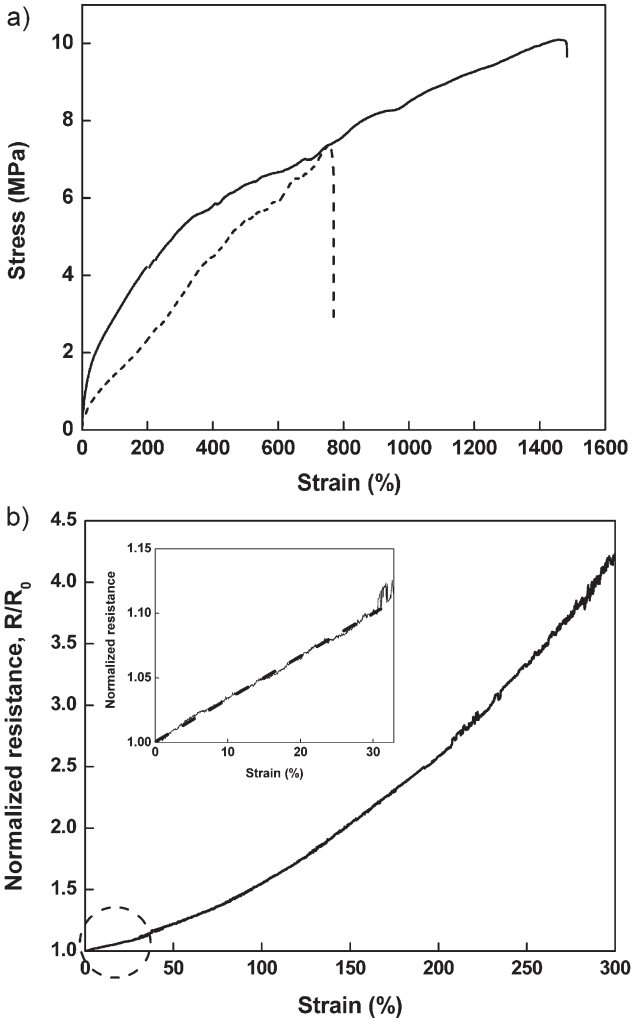

Figure 2. a) Plot of stress vs. strain for the forest/PU sheet (solid line) and the control PU sheet (dashed line) prepared using the same conditions. b) Dependence of normalized resistance (R/R_0) of the forest/PU composite sheet on the strain of elongation. The low strain region (dashed circle) is shown in the inset. The dashed red line is fit of the data with the straight line.

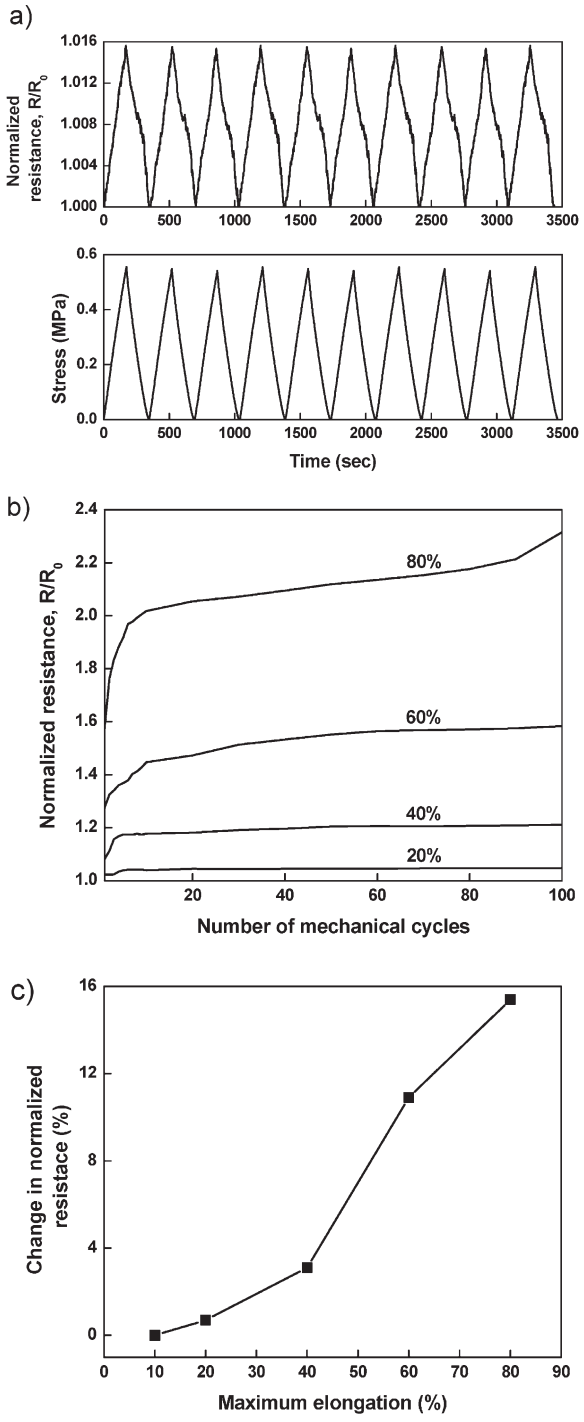

Figure 3. a) Normalized resistance (R/R_0) and applied stress for the forest/PU composite sheet vs. time during strain cycling between 0% and 10%. (b) Dependence of normalized resistance in unloaded state on the number of elongation-contraction cycles as a function of the maximum applied strain, which is indicated on the curves. (c) Change in normalized resistance shown in graph (b) in going from the 10^{th} to the 100^{th} cycle as a function of the maximum applied strain. The first 10 cycles for each strain set were used to provide initial sample conditioning.

the in-plane mechanical properties of an uninfiltrated nanotube forest would provide negligible contribution to these mechanical properties for the composite. The strain-to-failure for our composite was surprisingly high, over 1400%, which is much higher than the strain-to-failure for the reference pure PU sheet (about 760%). Like the modulus and strength, this evidences highly effective bonding between PU chains and the nanotubes in the MWNT forest.

The elongation upon loading was accompanied by an increase in the sheet electrical resistance R measured using a two-probe technique. The recorded values were normalized by the sample initial resistance R_0 at zero strain, and are shown in Figure 2b as a function of the applied stain. One can see that at relatively small strains (up to about 30%) the dependence of normalized resistance on percent strain is close to linear, with the slope of 0.34, as shown in the inset in Figure 2b. This slope increases with increasing strain to reach 1.07 at 300% strain (this value is the average slope from 0% to 300%).

The change in electrical resistance at stretching was found to be highly reversible in the low strain region. The high reversibility of the dependence of resistance on strain is illustrated in Figure 3a for a composite sheet subjected to cyclic 10% elongation and contraction. The dependence of relative resistance change on going from zero loading to maximum strain on the number of stretching cycles is shown in Figure 3b for maximum strains in the 20% to 80% range. One can see that the resistance change of the composite sheet stabilizes after the first 10 elongation/contraction cycles. After such initial conditioning, the resistance change of the composite remains almost constant for maximum strains that are not too high—the drift in resistance $\Delta R/R_0$ is less than 4% during the next 100 cycles for strains up to 40%. Cyclically straining the composite over 40% increases the irreversible component of cycling-induced resistance change, as shown in Figure 3c. These measurements evidence that the composite can be used as a strain sensor for the detection of moderate strains.

Electrical properties of prepared sheets revealed little sensitivity to twisting and bending deformations. Figure 4 shows that the resistance of the unloaded sheets remained nearly constant during numerous bending and twisting cycles. After some conditioning, the zero strain resistance of samples typically changed only by 1%–2% in the next 100 cycles. This evidences that the 3D structure of the MWNT forests in the PU matrix can effectively retain its original shape. The composite sheets will therefore work well in applications that require severe sensor bending or twisting, such as electronic textiles.

Unlike conventional CNT/polymer composites, forest–based sheets have a very large strain-to-failure (over 1400%), high electrical conductivity at quite small overall nanotube loading, and show highly reversible changes in resistance in the moderate strain range (up to 20%). In contrast, conventional CNT-based composites typically provide irreversible changes in resistance when cycled to such strain levels, which can be due to combinations of irreversible breaking of inter-nanotube interconnections and introduction of nanotube alignment. The results show that the forest-based composites are more resilient in structural retention upon stretching. This feature of the present composites can be related to their unique 3D forest derived structure, which can be seen in SEM images (Fig. 1c). The

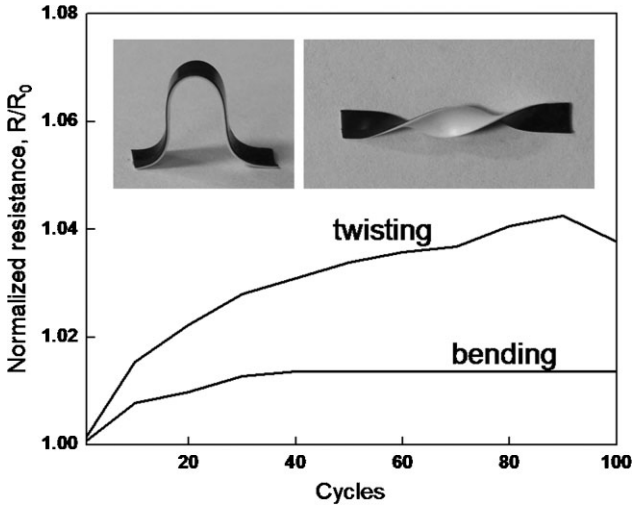

Figure 4. Dependence of zero strain resistance (R/R_0) on the number of bending and twisting cycles. The sample shape induced by bending and twisting is shown in the insets.

reversibility of electrical conductivity changes can be explained using an ''accordion'' model for the conducting carbon nanotube network (Fig. 5b) embedded in the highly elastic PU matrix. According to this model, the opening and closing of the ''accordion-like'' forest skeleton, held together with the PU binder, is responsible for the reversible elastic mechanical properties and electrical properties upon sheet elongation and contraction. Irreversible elastic and electrical changes occur only at relatively high strain levels. Also, retention of the three-dimensional nanotube interconnectivity of the initial forest to the forest/PU composites insures high electrical conductivity through percolation at low carbon nanotube levels.

It is known that electrical conductivity of CNT-based composites is controlled by the resistance of nanotubes and contacts between nanotubes at junction points that depend on the stress applied to the material. In conventional CNT-loaded polymer matrices, the stress to the junctions is transferred to large extent through stiff nanotube filler. Therefore, the resistance change is sensitive to small material deformations.[21] Extensive studies of the resistance-strain sensitivity, factors responsible for the conductivity of CNT-polymer films and corresponding models were reported previously.[22]

In the accordion-like forest structures, the stress to nanotubes and nanotube junctions is transferred mainly through highly elastic polymer binder surrounding the conductive nanotube network. Good coupling of conductive properties of the CNT network and elastic properties of polymer binder (rather than CNT filler) achievable in forest/PU sheets is responsible for the highly reproducible changes in the composite resistivity even at high strain levels.

In conclusion, highly elastic and electrically conductive composite sheets were prepared by infiltration of MWNT forests with PU binder. After pretreatment by initial cycling, the sheets provide highly reproducible changes in resistivity upon stretching for strains up to 40%. Almost no degradation in electrical properties and linear dependence of resistivity on strain was observed for strains in 10%–20% maximum range. The resistivity of the films showed little sensitivity to sheet twisting and bending. The properties of the composite were explained by the 3D accordion-like structure of a conductive carbon nanotube network held together with an elastic polymer binder. Because of the unique combination of high electrical and elastic properties, the forest-based composites can be used for high deformation strain sensors, conducting clothes, skin-like materials with self-sensing capabilities, and highly stretchable electrodes for actuators and artificial muscles.

Experimental

The aligned arrays of multiwalled carbon nanotubes (MWNT forests) were grown on a Si wafer using a conventional CVD method, as described in ref. [17]. The forest typically covered an area of about 50 cm^2 and had height of about 50 μm, as determined using conventional optical microscopy. The poly[4,4′-methylene-bis(phenyl isocyanate)-alt-1,4-butanediol/poly(butylene adipate)], referred to as polyurethane (PU), and DMF were purchased from Sigma-Aldrich (USA). Two grams of PU was dissolved in 20 g of DMF at room temperature with intense stirring. The prepared solution was then infiltrated into MWNT forests using a drop-casting technique. After evaporation of DMF, composite forest/PU sheets were mechanically peeled off the Si wafer, and cut into $20 \times 3 \times 0.25$ mm^3 strips. Three specimens of forest/PU composites were prepared and tested. The observed average values along with deviations for elastic modulus, mechanical strength, and elongation at break were 19.3 ± 0.2 MPa, 10.0 ± 0.2 MPa, and $1390\% \pm 70\%$, respectively. In the case of PU sheets prepared at the same conditions, elastic modulus, mechanical strength, and elongation at break were 7.8 ± 0.04 MPa, 7.3 ± 0.05 MPa, and $770\% \pm 30\%$, respectively.

Characterization: SEM images were taken using an LEO 1540 VP SEM. Two-probe electrical resistivity measurements were performed using a

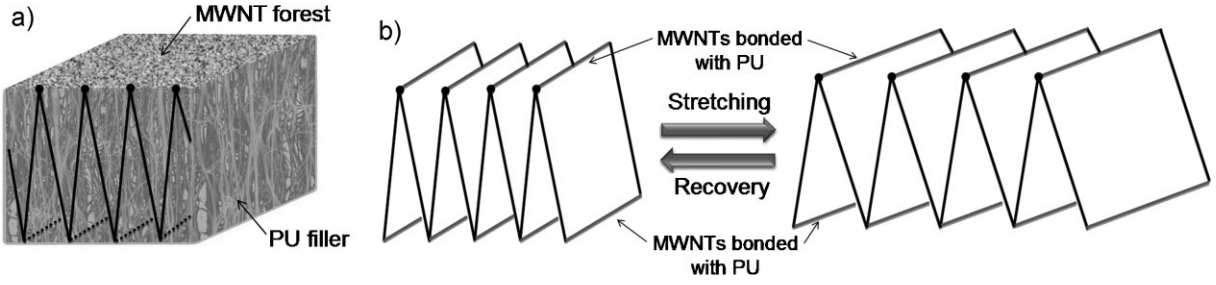

Figure 5. a) Model of the 3D accordion structure of a conducting MWNT forest network embedded into a PU matrix. b) A diagram showing stretching and recovery of the 3D accordion structure.

Keithley 2602 Sourcemeter connected to a computer. The data were acquired automatically as a function of applied strain. The stress vs. strain dependences were recorded using an Instron 5848 Micro Tester.

Acknowledgements

This work was supported by Creative Research Initiative Center for Bio-Artificial Muscle of the Ministry of Education Science and Technology (MEST) in Korea and NSF grant DMI-0609115 and Office of Naval Research MURI grant N00014-08-1-0654 in USA.

Received: December 14, 2009
Revised: January 25, 2010
Published online: May 5, 2010

[1] R. F. Service, *Science* **2003**, *301*, 909.
[2] M. Fihn, *Solid State Technol.* **2006**, *49*, 43.
[3] S. P. Lacour, J. Jones, Z. Suo, S. Wagner, *IEEE Electron Device Lett.* **2004**, *25*, 179.
[4] J. M. Engel, N. Chen, K. Ryu, S. Pandya, C. Tucker, Y. Yang, C. Liu, in *Solid State Sensors, Actuators, and Microsystems Workshop* (Eds: L. Spangler, T. W. Kenny), Transducer Research Foundation, San Diego, CA **2006**, p. 316.
[5] L. Johnson, F. K. Perkins, T. O'Hearn, P. Skeath, C. Merritt, J. Frieble, S. Sadda, M. Humayun, D. Scribner, *J. Neurosci. Methods* **2004**, *137*, 265.
[6] R. Pelrine, R. Kornbluh, Q. B. Pei, J. Joseph, *Science* **2000**, *287*, 836.
[7] R. Pelrine, R. Kornbluh, G. Kofod, *Adv. Mater.* **2000**, *12*, 1223.
[8] D. Y. Khang, H. Q. Jiang, Y. Huang, J. A. Rogers, *Science* **2006**, *311*, 208.
[9] Y. G. Sun, W. M. Choi, H. Q. Jiang, Y. G. Y. Huang, J. A. Rogers, *Nat. Nanotechnol.* **2006**, *1*, 201.
[10] D.-H. Kim, J.-H. Ahn, W. M. Choi, H.-S. Kim, T.-H. Kim, J. Song, Y. Y. Huang, Z. Liu, C. Lu, J. A. Rogers, *Science* **2008**, *320*, 507.
[11] T. Sekitani, Y. Noguchi, K. Hata, T. Fukushima, T. Aida, T. Someya, *Science* **2008**, *321*, 1468.
[12] Q. Cao, H. Kim, N. Pimparkar, J. P. Kulkarni, C. Wang, M. Shim, K. Roy, M. A. Alam, J. A. Rogers, *Nature* **2008**, *454*, 495.
[13] V. K. Rangari, M. Yousuf, S. Jeelani, M. X. Pulikkathara, V. N. Khabashesku, *Nanotechnology* **2008**, *19*, 245703.
[14] P. G. Whitten, G. M. Spinks, G. G. Wallace, *Carbon* **2005**, *43*, 1891.
[15] M. Zhang, K. R. Atkinson, R. H. Baughman, *Science* **2004**, *306*, 1358.
[16] K. Koziol, J. Vilatela, A. Moisala, M. Motta, P. Cunniff, M. Sennett, A. Windle, *Science* **2007**, *318*, 1892.
[17] M. Zhang, K. R. Atkinson, R. H. Baughman, *Science* **2004**, *306*, 1358.
[18] N. G. Sahoo, Y. C. Jung, H. J. Yoo, J. W. Cho, *Compos. Sci. Technol.* **2007**, *67*, 1920.
[19] J. W. Cho, J. W. Kim, Y. C. Jung, N. S. Goo, *Macromol. Rapid Commun.* **2005**, *26*, 412.
[20] F. Li, L. Qi, J. Yang, M. Xu, X. Luo, D. Ma, *J. Appl. Polym. Sci.* **2000**, *75*, 68.
[21] M. Park, H. Kim, J. P. Youngblood, *Nanotechnology* **2008**, *19*, 055705.
[22] X. Song, S. Liu, Z. Gan, Q. Lv, H. Cao, H. Yan, *Microelectron. Eng.* **2009**, *86*, 2330.